ELSEVIER

Journal of Alloys and Compounds 275–277 (1998) 41–45

Journal of ALLOYS AND COMPOUNDS

Rare earth iron garnets and rare earth iron binary oxides synthesized by microwave monomode

M. Gasgnier[a,*], J. Ostoréro[b], A. Petit[a]

[a]*Laboratoire des Réactions Sélectives Sur Support, URA CNRS 478, ICMO, Bat. 410, Université Paris-Sud, F-91405 Orsay Cedex, France*
[b]*CNRS, Laboratoire de Chimie Métallurgique et Spectroscopie des Terres Rares, UPR 209, 1 Place A. Briand, F-92195 Meudon Cedex, France*

Abstract

Rare earth iron garnets ($R_3Fe_5O_{12}$ or RIG, with R=Y, Sm, Eu, Gd, Dy, Ho, Er, and Yb) and rare earth orthoferrites $RFeO_3$ have been synthesized from R_2O_3/Fe_3O_4 mixtures using the monomode microwave (MW) method. Such binary compounds are formed at a low temperature ($T<900$ K), in a few minutes at ambient atmosphere, whereas under conventional solid state reactions, all these binary oxides are synthesized at a much higher temperature (~1800 K). The experimental conditions leading to nearly pure RIG are briefly discussed in relation to the nature of the rare earth and to the ratio R_2O_3/Fe_3O_4 in the starting mixture. This experimental method was extended to the synthesis of lanthanum- and cerium-doped yttrium iron garnet compounds. These results show that MW is a practical and economical procedure for chemical syntheses. © 1998 Elsevier Science S.A.

Keywords: Microwave; Synthesis; Rare earth iron garnets

1. Introduction

Rare earth iron garnets (RIG or $R_3Fe_5O_{12}$) constitute a very important class of materials due to their magnetic and magnetooptic properties [1]. Numerous works have been devoted to the synthesis of these compounds in bulk polycrystalline or single crystals as well as thin films. The classical solid-state reactions involve high-temperature procedures (T~1500–1800 K), lengthy sintering time (several hours) and grinding steps between R_2O_3 and α-Fe_2O_3. It has been previously demonstrated [2–5] that such syntheses can be hastened at low temperature (T~800–900 K) with a reaction time of the order of few minutes, at ambient atmosphere, by using a monomode microwave (MW). In this case, the syntheses were carried out with Y_2O_3/Fe_3O_4 mixtures which allowed to form yttrium iron garnet YIG [2], yttrium orthoferrite $YFeO_3$ and, surprisingly, the YFe_2O_4 compound [2], which is synthesized at high temperature and low oxygen pressure (10^{-10} atm) under classical solid-state reactions [6]. Lastly, it has been also observed that there is always formation of α-Fe_2O_3 [2,3] and sometimes of FeO and Fe during the MW treatment [2]. In this study, we have extended our investigations to the rare earth series leading to pure $R_3Fe_5O_{12}$ (from Sm to Yb, except Tb and Tm), and to La and Ce substitutions to yttrium in YIG compounds, where pure La and Ce iron garnets do not exist.

2. Experimental

The experimental procedure has been described in more detail in previous papers [2–5]. The MW apparatus (Prolabo Cy., Maxidigest 350), is equipped with a magnetron having the following characteristics: $f=2.45$ GHz ($\lambda=12.2$ cm), $P=300$ W. The recorded temperature is measured by a IR pyrometer located inside the MW. Accurate measurements carried out with a special low-temperature IR pyrometer have shown a temperature shift of 50–80 K compared to the first pyrometer [3].

Fe_3O_4 (Johnson Mathey 99.99%) and R_2O_3 (from different manufacturers, 99.9% at least) powders were used as starting materials. Different compositions of R_2O_3/Fe_3O_4 mixtures were studied with a metallic ratio $r=R/Fe=3/[5(1+x)]$ ($x=0$, 10 and 20%) in the vicinity of 0.6 corresponding to the stoichiometric garnet compound. Each mixture is poured into a glass or quartz tube which is rotating (~30 rpm) during exposure to MW beam.

X-ray diffraction (XRD) experiments are performed on the different parts of the reacted samples: hard melted aggregates and the remaining powder. It is to be noted that, in contrast to our previous experiments on YIG synthesis

*Corresponding author.

0925-8388/98/$19.00
PII: S0925-8388(98)00270-9

using the MW method [2], all these different components could not be magnetically separated at room temperature.

3. Results and discussion

All the results and observations are reported in Table 1.

3.1. MW synthesis

According to the nature of the rare earth and to the composition of the starting charge, the behaviour of the mixed oxide powders under MW exposure are quite different. Typical temperature versus time curves recorded during MW experiments are presented in Fig. 1 (Dy (x=10%); Sm (x=10%) and Yb (x=20%)) and Fig. 2 (Ho (x=10%) and Yb (x=10%)). The numbers in parentheses correspond to the excess of Fe_3O_4 (x, %) in the starting

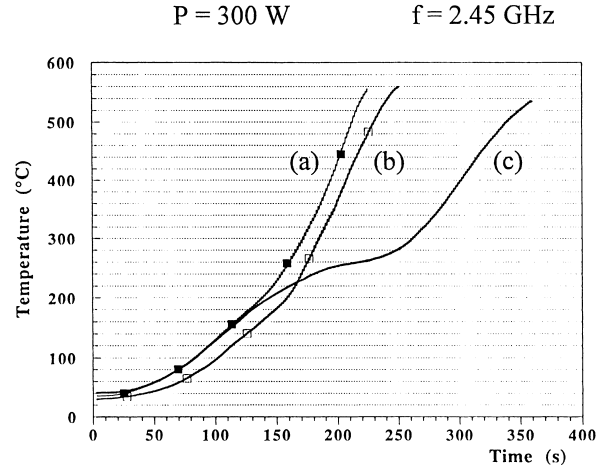

Fig. 1. Temperature versus time curves during MW heating of R_2O_3/Fe_3O_4 mixtures for: (a) R=Dy (x=10%); (b) Sm (x=10%); (c) Yb (x=20%).

Table 1
Approximate compositions (%) of the different binary rare earth and Fe oxides synthesized after MW exposure

R	x (%)	Melted part	Unmelted powder	Starting red hot	Light flashes, burstings	Remarks
Y	0	YIG(50) $YFeO_3$ (50)	α-Fe_2O_3 Y_2O_3	~523 K (white hot 875 K)	Yes	Powders become red
	10	YIG (90) $YFeO_3$ (10)	α-Fe_2O_3 Y_2O_3	~523 K (white hot 875 K)	Yes	Synthesis of YFe_2O_4
Y/Sc=2/1	10	$Y_3Fe_{5-t}Sc_tO_{12}$	α-Fe_2O_3 Y_2O_3, Sc_2O_3	~523 K	Yes	a_0=1.2463 nm; t=1
Y/La=2/1	10	$Y_{3-z}La_zFe_5O_{12}$ (90) $YFeO_3$:La (10)	Y_2O_3, $LaFeO_3$, Fe_3O_4	~523 K (white hot 773 K)	Yes	a_0=1.2427 nm; z=0.46 (classical limit z=0.5)
Y/Ce=2/1	0	$Y_{3-z}Ce_zFe_5O_{12}$ (90) $YFeO_3$:Ce (10)	Y_2O_3, CeO_2, α-Fe_2O_3	~523 K	Yes	a_0=1.2414 nm; z~0.21 (classical limit z~0.08)
Sm	0	$SmFeO_3$ (75) SmIG (25)	Sm_2O_3, α-Fe_2O_3	~523 K (white hot 873 K)	Yes	H_2O condensation on tube wall
	10	SmIG (50) $SmFeO_3$(50)	Sm_2O_3, α-Fe_2O_3	473 K	Yes	A few big melted blocks
Eu	10	EuIG (80) $EuFeO_3$ (20)	α-Fe_2O_3 Eu_2O_3	~593 K	Yes	
Gd	0	$GdFeO_3$ (50) Gd_2O_3 (40) GdIG (10)	α-Fe_2O_3 Gd_2O_3	573 K	Yes	Few small melted aggregates
	10	GdIG (90) $GdFeO_3$ (10)	α-Fe_2O_3 Gd_2O_3	523 K	Yes	Few unmelted powder
Dy	10	DyIG (>90) $DyFeO_3$ (<10)	Dy_2O_3 α-Fe_2O_3	653 K	Yes	Few small melted aggregates
Ho	0	$HoFeO_3$ (80) HoIG (15) Fe_3O_4 (5)	Ho_2O_3 α-Fe_2O_3	No	No	Few small melted aggregates
	10	No	Ho_2O_3 α-Fe_2O_3	No	No	'Magnetic' red powder
Er	0	ErIG (40) $ErFeO_3$ (60)	α-Fe_2O_3 Er_2O_3 ErIG	No	No	Few small melted aggregates
	10	ErIG (45) $ErFeO_3$ (55)	α-Fe_2O_3 Er_2O_3 ErIG	No	No	Few small melted aggregates
Yb	10	No	Yb_2O_3 α-Fe_2O_3	No	No	'Magnetic' red powder
	20	YbIG (80) $YbFeO_3$ (20)	Yb_2O_3 α-Fe_2O_3	493 K	Yes	Few unmelted powder

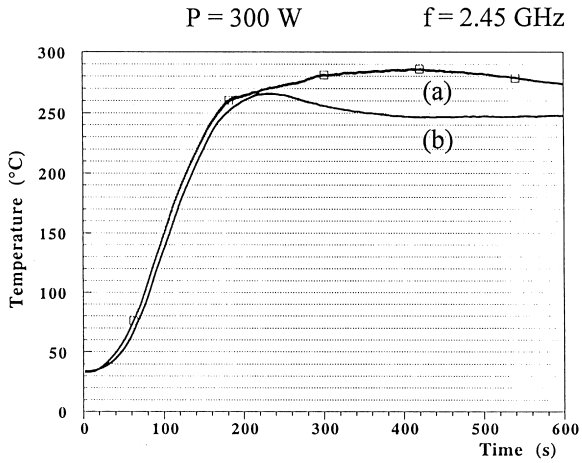

Fig. 2. Temperature versus time curves during MW heating of R_2O_3/Fe_3O_4 mixtures for: (a) R=Ho (x=10%); (b) Yb (x=10%).

mixture as compared to the stoichiometric garnet. It has been observed [4] that pure Fe_3O_4 powder is quickly heated at the impact of the MW beam. For instance, 5 g weight becomes red-hot in less than 30 s, and white-hot in less than 1 min. In this way, as R_2O_3 powders do not absorb efficiently the MW beam [4,5], it was observed that a Fe_3O_4 excess enhanced the chemical reaction [2].

Fig. 1 corresponds to the cases where the reaction leads to the synthesis of melted binary oxides. The curves present an exponential shape and the reaction is accompanied by a number of light and acoustic phenomena: when the mixture powder becomes red hot, strong burstings are heard and, simultaneously, white, red and purple flashes are already observed. Then the powder becomes incandescent white. At this moment, hard black melted blocks are formed. Lastly, the part of the sample powder which has not transformed into melted aggregates takes a red colour. This is in contrast to the oxide mixtures corresponding to Fig. 2: the powders did not turn red hot, and the temperature versus time curves present a plateau (~523 K) after a MW treatment of about 3 min. No light or acoustic phenomena occur. After the MW exposure, the resulting powder presents a red colour. Surprisingly, this red powder, the colour of which is typical of α-Fe_2O_3 compound, is 'magnetic', that is to say, attracted by a magnet at room temperature. At the macroscopic scale, XRD patterns reveal only the coexistence of α-Fe_2O_3 and R_2O_3 (Fig. 3).

The powders were crushed in a mortar to be studied by a transmission electron microscope. In the case of the Ho_2O_3/α-Fe_2O_3 mixture, electron diffraction patterns show the coexistence of the two basal compounds and of a third one. Among the various iron oxides, it was possible to identify this phase as tetragonal γ_T-Fe_2O_3 (ICDD-JCPDS card # 25-1402). Compared to magnetic γ_C-Fe_2O_3 spinel lattice, the tetragonal one is characterized such as: $a_T=a_C=0.834$ nm, $c_T=3a_C=2.502$ nm. To our knowledge, the magnetic properties of the γ_T phase have not been reported elsewhere. In the case of the Yb_2O_3/α-Fe_2O_3 mixture (x=10%), once again the three phases are observed on electron diffraction patterns. However, other ones reveal the presence of small particles. The calculated

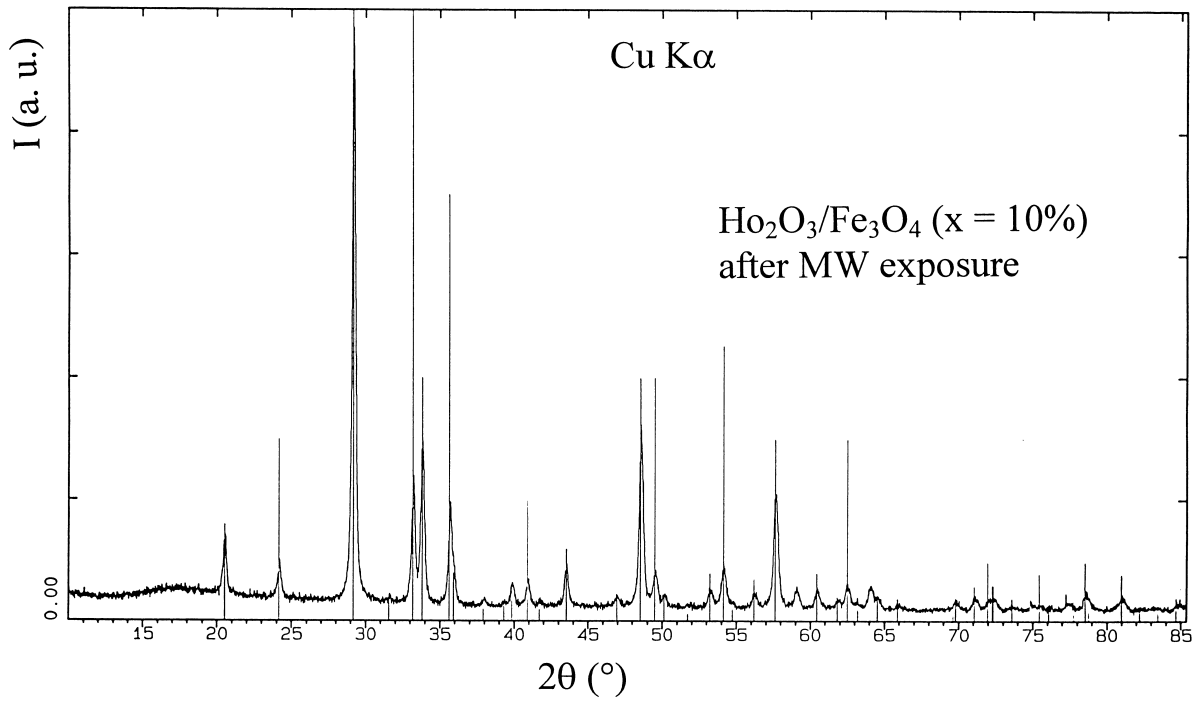

Fig. 3. XRD patterns of the resulting powder Ho_2O_3/Fe_3O_4 (x=10%) after MW exposure. All the lines correspond to a mixture of Ho_2O_3 (ICDD-JCPDS card # 10-0194) and α-Fe_2O_3 (ICDD-JCPDS card # 33-0664).

interplanar spacings should be consistent with another iron oxide: rhombohedral β-Fe_2O_3 (ICDD-JCPDS card # 40-1139) of which the parameters are such as: $\sqrt{2}a_R = a_C$ and $c_R = 6\sqrt{2}a_C$.

Such observations should explain the magnetic behavior of the powders after MW exposure: seeds of magnetite, γ_C-Fe_2O_3, or derived phases (γ_T-Fe_2O_3, β-Fe_2O_3) may be inserted at the heart of the R_2O_3/α-Fe_2O_3 particles.

3.2. X-ray diffraction analyses

From Table 1, it appears that the mixtures presenting a MW behaviour similar to Fig. 2 are mainly represented by the heavier rare earth (Ho, Er, Yb) oxides and an Fe_3O_4 excess, $x=0$ or 10%. They correspond also mainly to the rare earth leading to the less—or no apparent—RIG formation. The influence of the R/Fe ratio is best evidenced for ytterbium. For $x=10\%$, the temperature versus time curve is presented in Fig. 2a; no binary oxides are apparently synthesized. For $x=20\%$, the temperature versus time curve is presented in Fig. 1c and YbIG (~80% pure) is obtained.

It seems, therefore, that RIG is synthesized quite easily from Sm to Dy with $x=0$ or 10%; whereas for the heavier rare earth (Ho, Er, and Yb) such a reaction needs a higher Fe_3O_4 excess to occur. Nearly pure RIG are obtained when $x=10\%$ (Eu to Dy). The XRD patterns show that the ferrimagnetic garnets are well crystallized and that the amount of other binary oxides is low (Fig. 4).

Concerning the other binary oxides, in contrast to previous experiments with Y_2O_3/Fe_3O_4 mixtures, only the rare earth orthoferrites $RFeO_3$ were observed. Particularly, RFe_2O_4 (R=Ho, Er and Yb [7–9]) isomorphous compounds of YFe_2O_4 synthesized during MW formation of YIG [2], are not observed in the XRD patterns of the different reaction products. The formation of binary Yb and Fe oxides like $Yb_2Fe_3O_7$ [10,11], $Yb_3Fe_4O_{10}$ and $Yb_4Fe_5O_{13}$ [12] has not been equally observed in our experimental conditions. This indicates that their amount, if any, is very low (less than a few %).

Finally, concerning the lighter rare earths, La and Ce, their pure iron garnets do not exist and we have to perform experiments on yttrium-substituted iron garnet materials. From XRD patterns and as indicated in Table 1, La and Ce substitute to yttrium to synthesize $Y_{3-z}R_zFe_5O_{12}$. Concerning YIG:La, the lattice parameter of the synthesized compound indicates that $z=0.46$ which is close to the limit $z=0.5$ where two phases are formed [13]. Another interesting result concerns YIG:Ce (Fig. 5). Assuming that Ce enters the garnet lattice as Ce^{3+} ions, the lattice constant of the synthesized garnet $a_0=1.2414$ nm, indicates that the amount of Ce substituted in YIG is $z=0.21$ [14,15]. This Ce concentration is much higher (~2.5 times) than the limit amount of this rare earth when synthesized using classical solid-state reactions (z~0.08) [16].

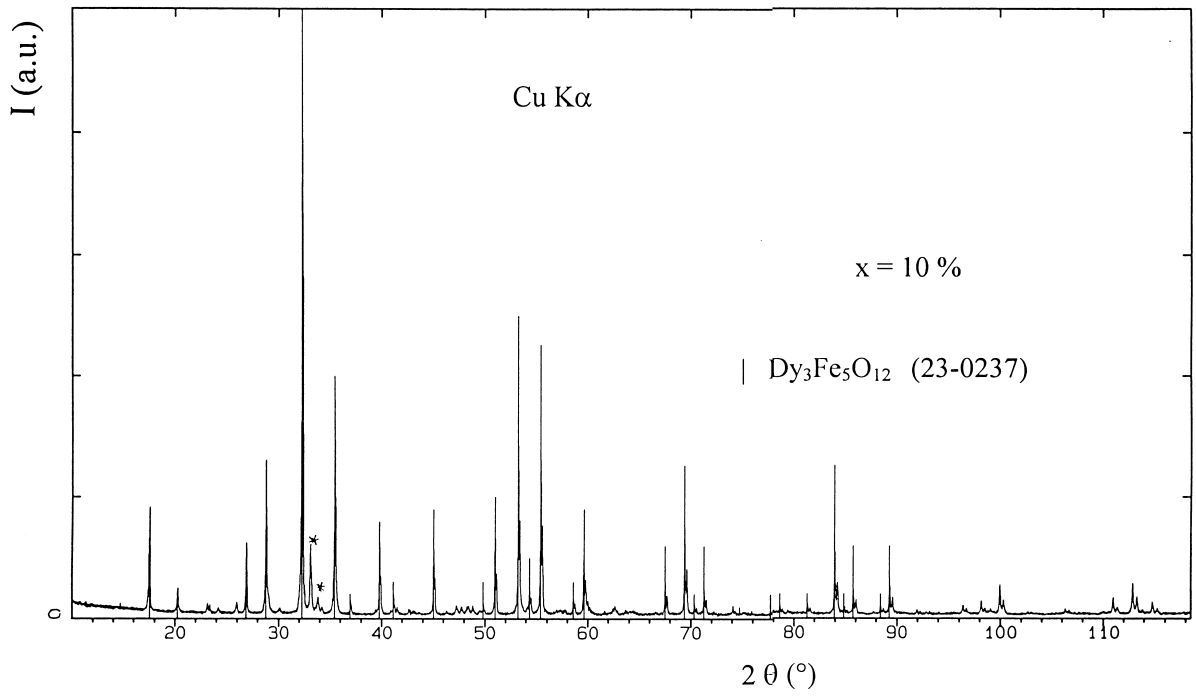

Fig. 4. XRD patterns of the melted aggregates after MW exposure of the mixture Dy_2O_3–Fe_3O_4 with $x=10\%$. The spectrum corresponds mainly to pure $Dy_3Fe_5O_{12}$ ferrimagnetic garnet (vertical bars, ICDD-JCPDS card # 23-0237). Small amounts of $DyFeO_3$ (stars) are also observed.

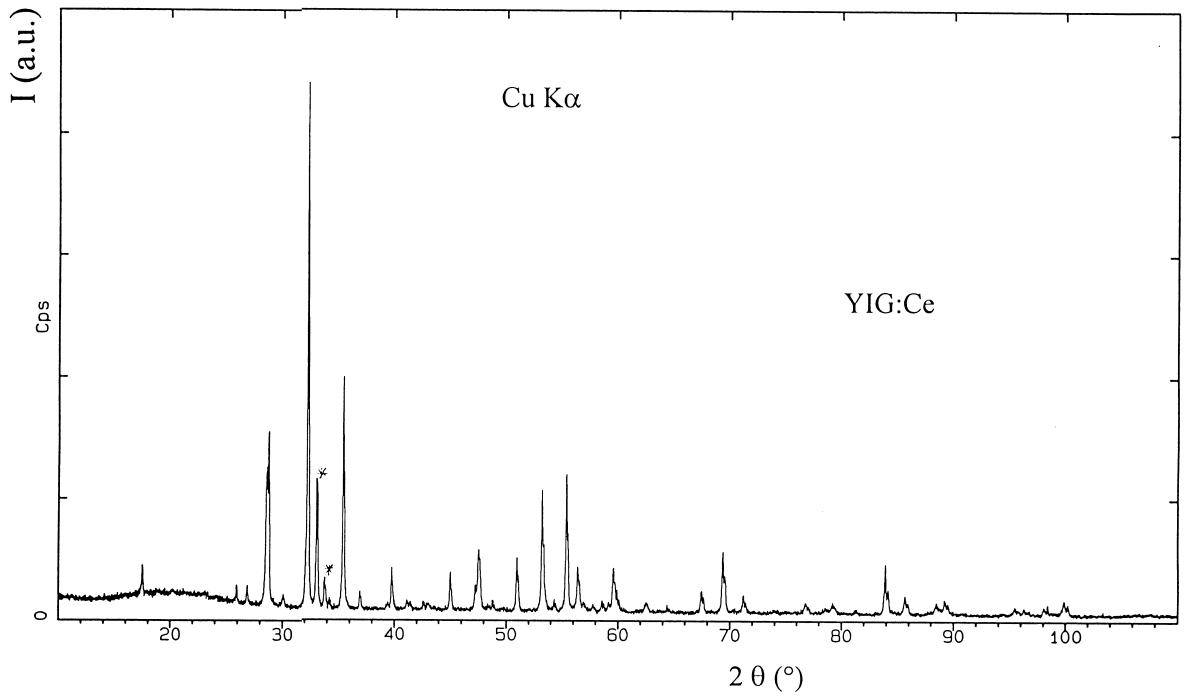

Fig. 5. XRD patterns of the melted aggregates after MW exposure of the mixture Y_2O_3–CeO_2–Fe_3O_4. The spectrum corresponds mainly to $Y_{3-z}Ce_zFe_5O_{12}$ ferrimagnetic garnet with a_0=1.2407 nm. Small amounts of $YFeO_3$:Ce are also observed (stars).

4. Conclusion

We have shown that it is possible to synthesize well-crystallized polycrystalline RIG (R=Sm to Dy) at low temperature (T<900 K) in a few minutes by means of a monomode MW treatment in air of mixed R_2O_3/Fe_3O_4 powders with an excess, x=0–10%, of Fe_3O_4 in relation to stoichiometric garnet. These experimental conditions are close to those determined for YIG synthesis [2]. The presence of some amounts of impurities ($YFeO_3$ or R_2O_3) in the case of nearly pure garnets (YIG, DyIG, GdIG, YIG:La or Ce) is essentially due to the fact that the heating was stopped before the reaction was fully achieved. Concerning the heavier rare earths (Ho to Yb), the synthesis of pure RIG seems to occur only for higher x values (x=20% in the case of Yb). Such a procedure allows also to obtain doped YIG where yttrium is partially substituted by La or Ce. In this latter case the amount of incorporated Ce is much higher than that obtained using conventional solid-state methods. Lastly, the magnetic behavior of the R_2O_3/α-Fe_2O_3 (R=Ho, Er, Yb) powders will be studied in order to correlate the electron microscopy results.

References

[1] J. Ostoréro, M. Escorne, J. Gouzerh, H. Le Gall, J. Phys. IV Colloques C1 (1997) 719.
[2] J. Ostoréro, M. Gasgnier, A. Petit, J. Alloys Compounds 262–263 (1997) 275.
[3] M. Gasgnier, A. Petit, H. Jullien, A. Loupy, Mater. Res. Bull. 31 (1996) 1101.
[4] M. Gasgnier, L. Albert, J. Derouet, L. Beaury, A. Loupy, A. Petit, P. Jacquault, J. Alloys Compounds 198 (1993) 73.
[5] M. Gasgnier, A. Loupy, A. Petit, H. Jullien, J. Alloys Compounds 204 (1994) 165.
[6] N. Kimizuka, T. Katsura, J. Solid State Chem. 13 (1975) 176.
[7] O. Evrard, B. Malaman, F. Jeannot, N. Tannières, J. Aubry, C.R. Acad. Sci. Paris C278 (1974) 413.
[8] K. Kitayama, T. Katsura, Bull. Chem. Soc. Jpn. 49 (1976) 998.
[9] N. Kimizuka, E. Takayama, J. Solid State Chem. 40 (1981) 109.
[10] O. Evrard, B. Malaman, N. Tannières, F. Jeannot, J. Aubry, C.R. Acad. Sci. Paris C279 (1974) 1021.
[11] B. Malaman, O. Evrard, N. Tannières, A. Courtois, J. Protas, Acta Crystallogr. B32 (1976) 749.
[12] N. Kimizuka, K. Kato, I. Shindo, I. Kawada, Acta Crystallogr. B32 (1976) 1620.
[13] G. Winkler, P. Hansen, P. Holst, Philips Res. Rep. 27 (1972) 151.
[14] S. Mino, A. tate, T. Uno, T. Shintaku, A. Shibukawa, Jpn. J. Appl. Phys. 32 (1993) 3154.
[15] Y. Okamura, J. Kubota, S. Yamamoto, IEEE Trans. Mag. 31 (1995) 3289.
[16] K.P. Belov, N.V. Volkova, V.I. Raitsis, Sov. Phys. Solid State 15 (1973) 612.